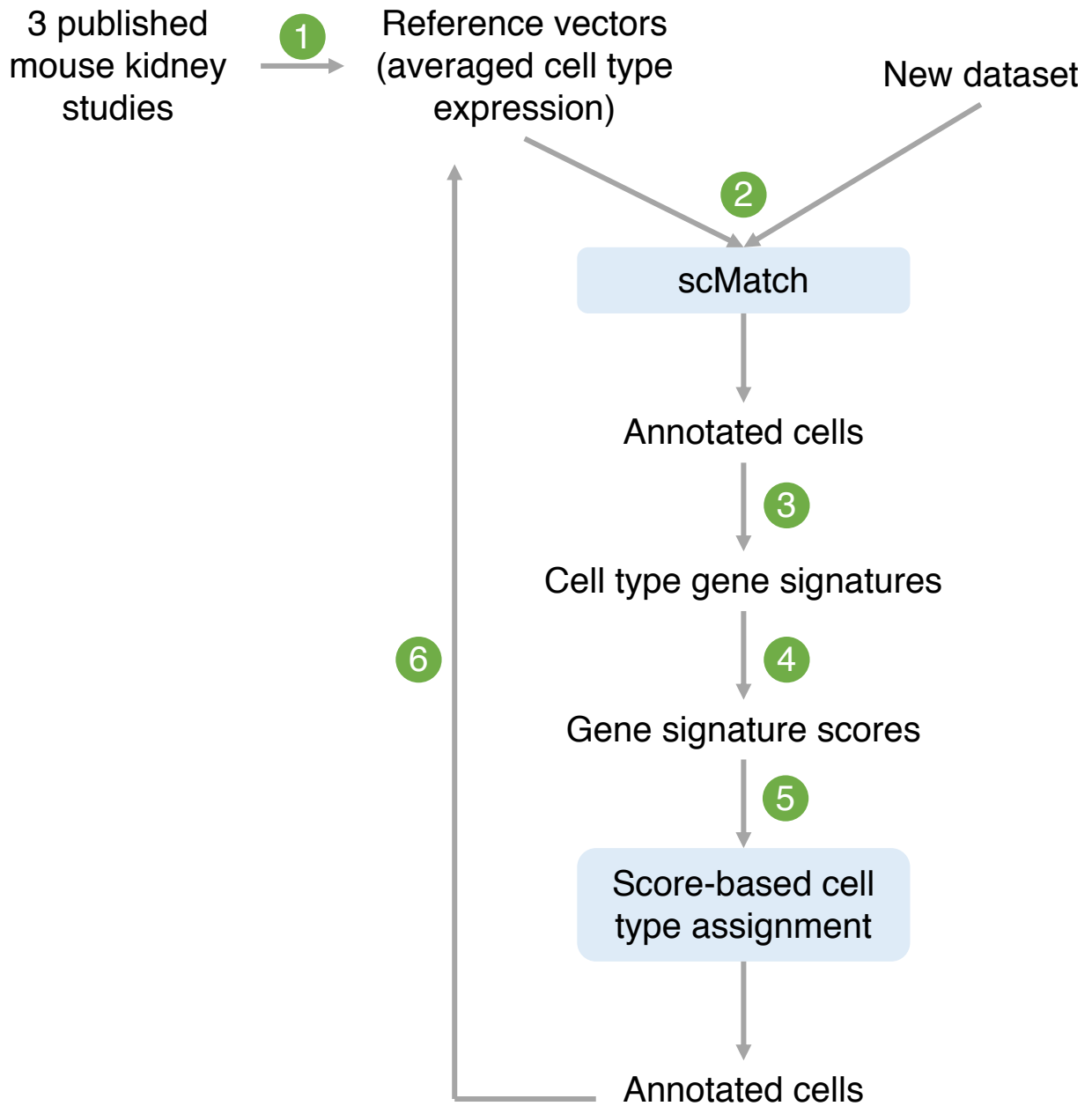
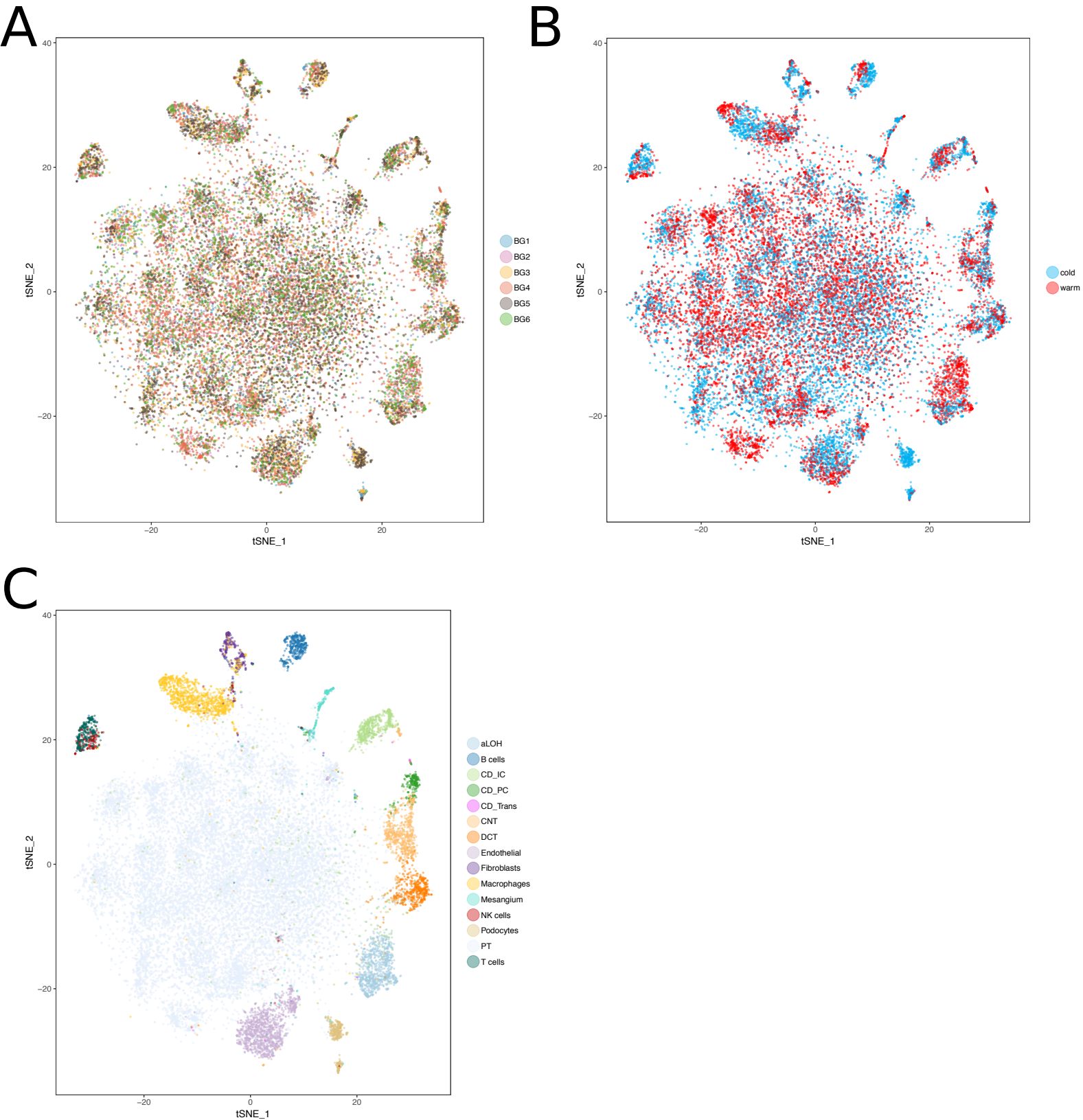


Fig. S1



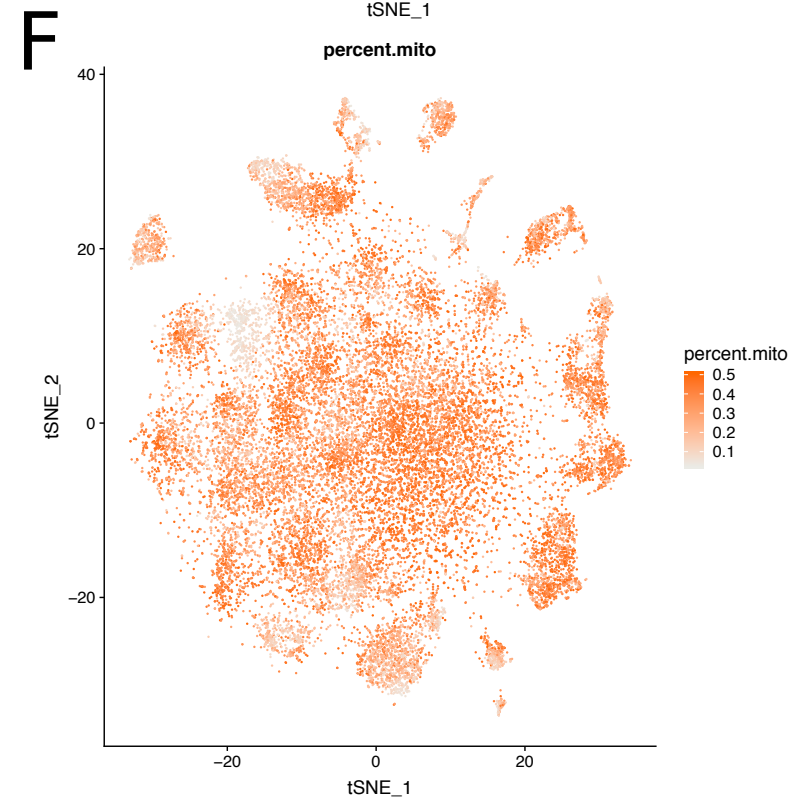
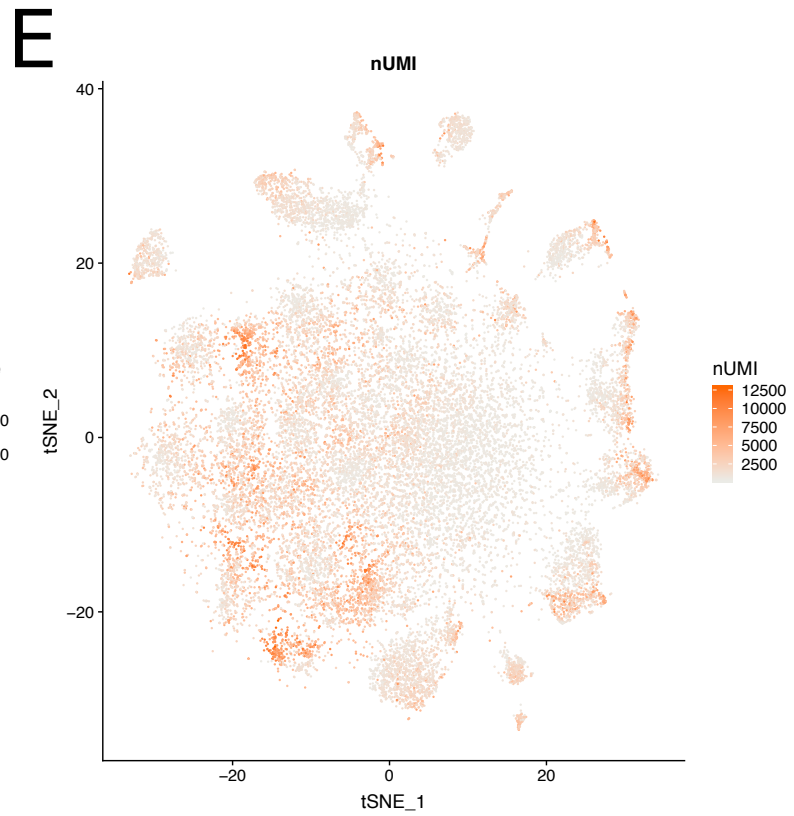
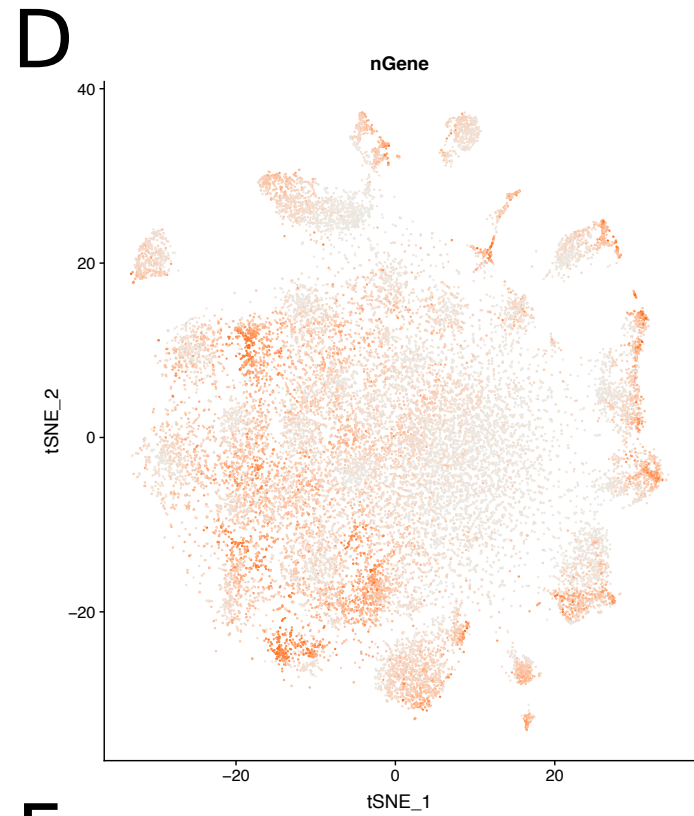
Cell annotation procedure. See **Methods** for more details.

Fig. S2



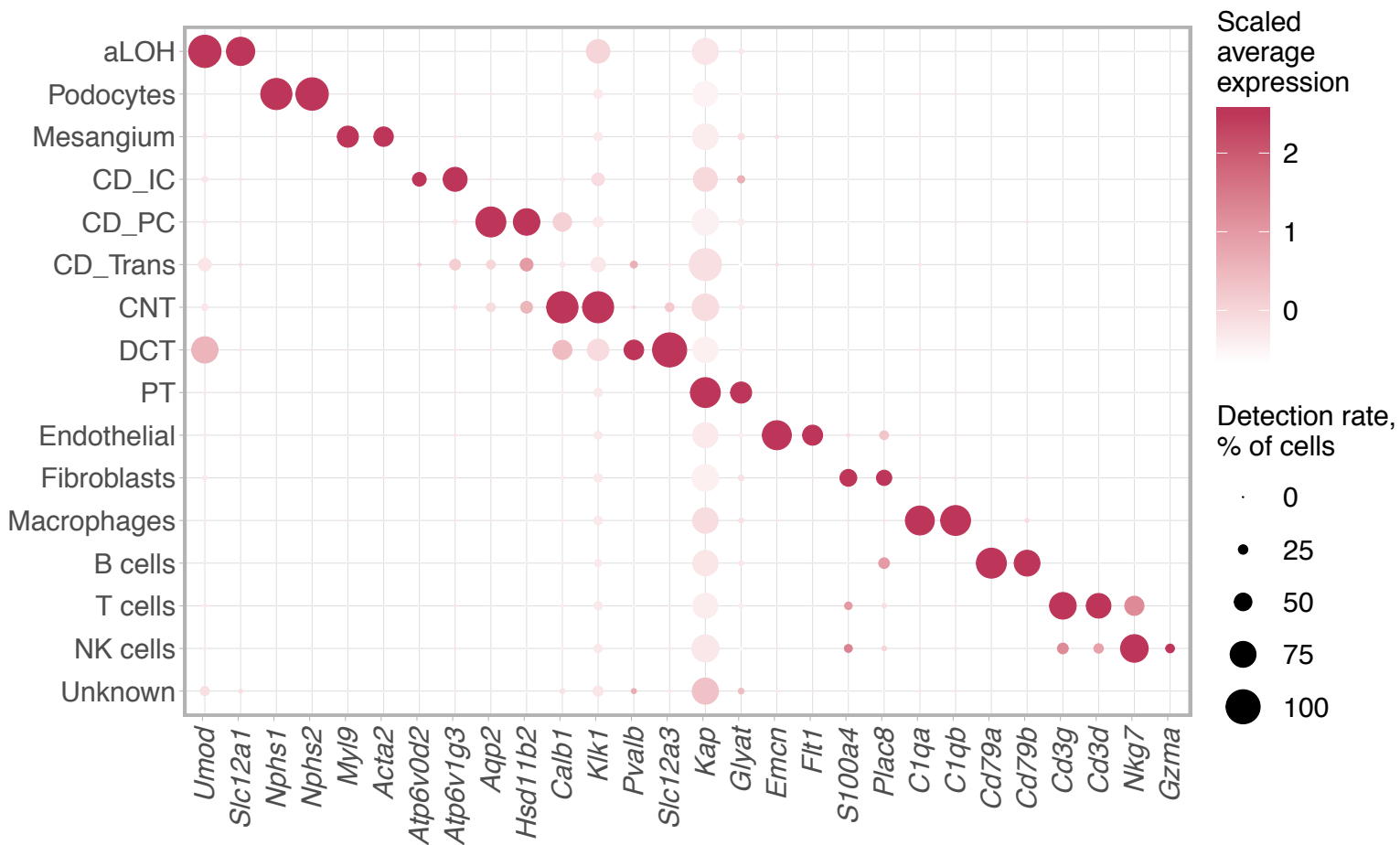
TSNE plots showing freshly profiled cells from cold- and warm-dissociated kidneys coloured by **a)** library, **b)** dissociation protocol, **c)** inferred cell type.

aLOH: ascending loop of Henle; CD_IC: intercalated cells of collecting duct; CD_PC: principal cells of collecting duct; CD_Trans: transitional cells of collecting duct; CNT: connecting tubule; DCT: distal convoluted tubule; PT: proximal tubule.



TSNE plots showing freshly profiled cells from cold- and warm-dissociated kidneys coloured by **d**) number of detected genes, **e**) number of UMIs, **f**) fraction of reads mapped to mitochondrial genes.

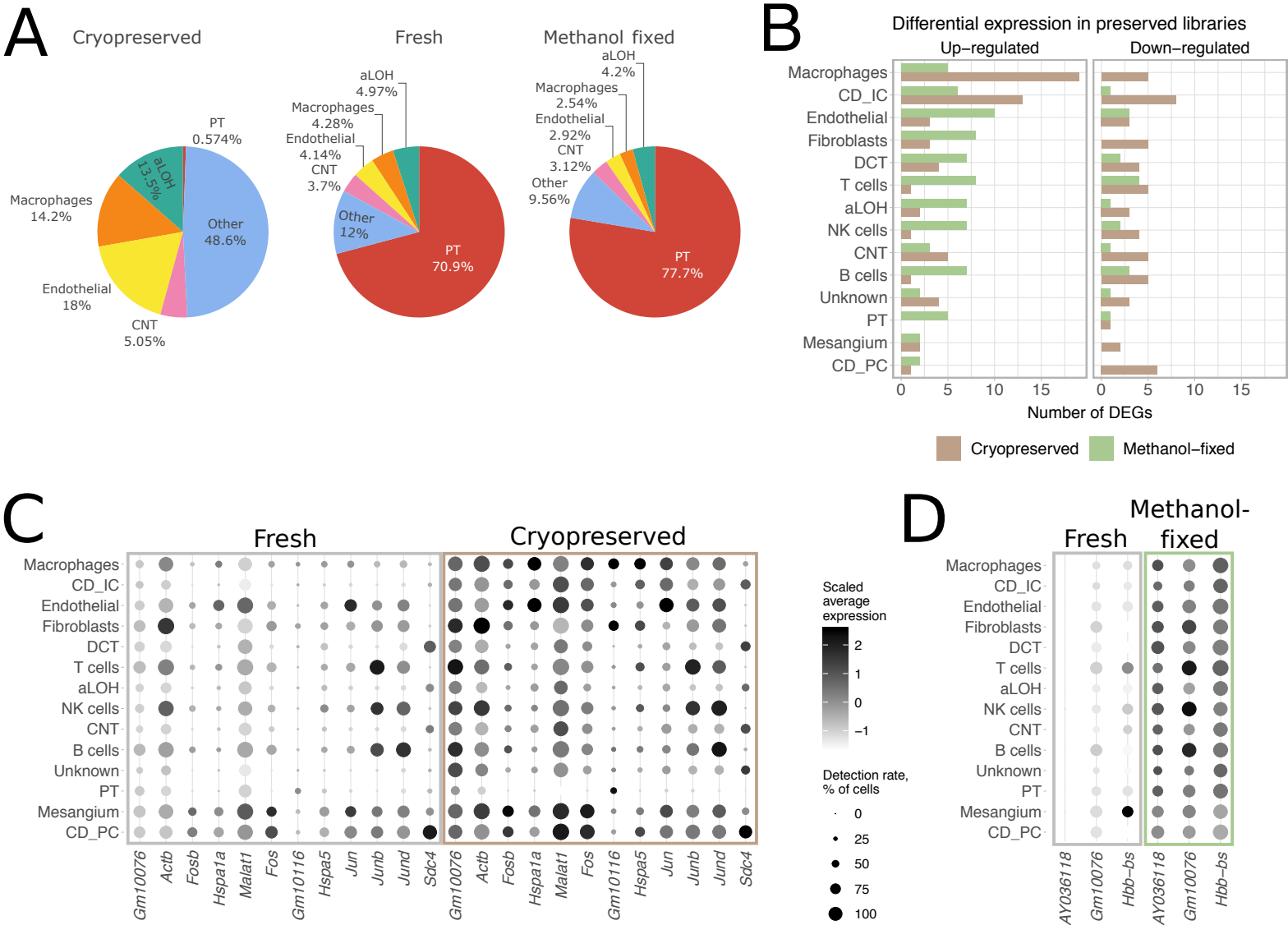
Fig. S3



Expression and detection levels of selected marker genes.

aLOH: ascending loop of Henle; CD_IC: intercalated cells of collecting duct; CD_PC: principal cells of collecting duct; CD_Trans: transitional cells of collecting duct; CNT: connecting tubule; DCT: distal convoluted tubule; PT: proximal tubule.

Fig. S4

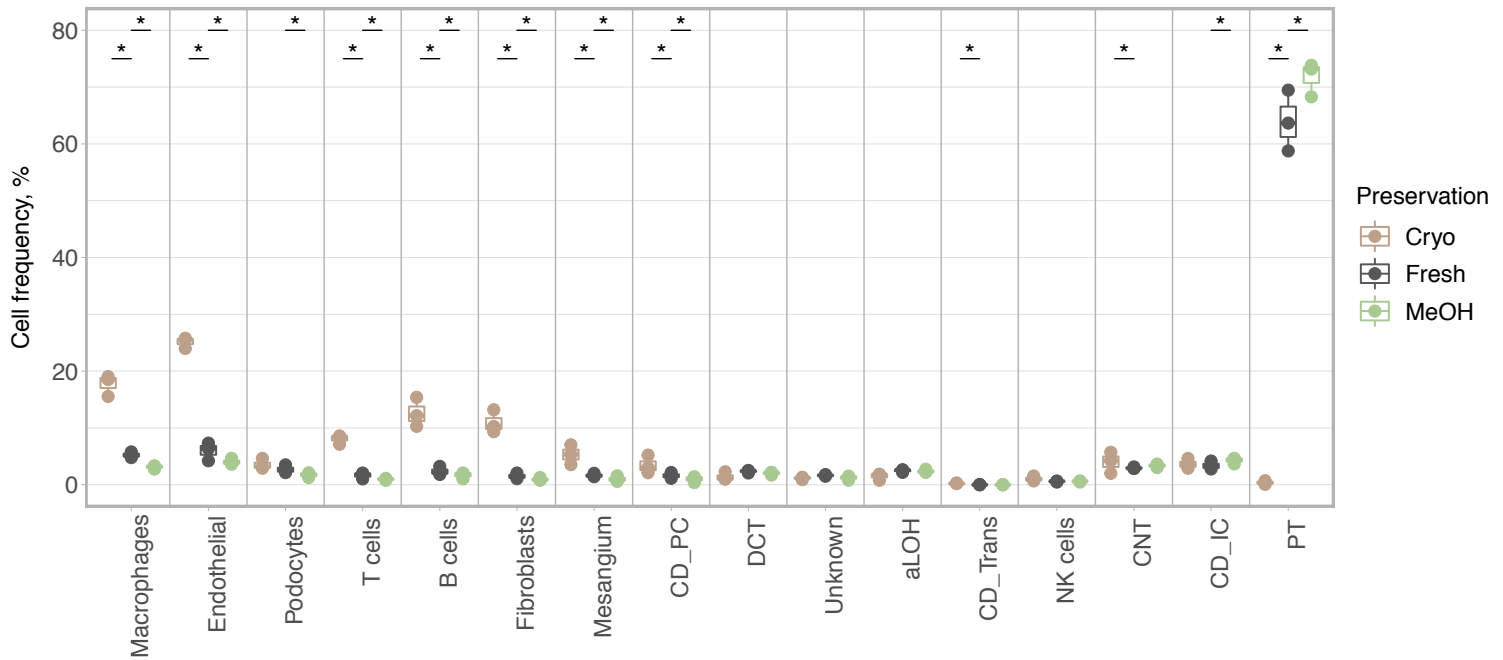


Cell preservation protocol performance in warm-dissociated samples. **a)** Cell type composition of fresh and preserved warm-dissociated samples. **b)** Number of DEGs detected between preserved and freshly profiled aliquots. Seurat Wilcoxon test with $\log_{FC} = 1$, min detection rate 0.5, $FDR < 0.05$ as thresholds. **c)** Expression and detection rates of DEGs with higher expression in cryopreserved samples in at least two cell types. **d)** Expression and detection rates of DEGs with higher expression in methanol-fixed samples in at least nine cell types.

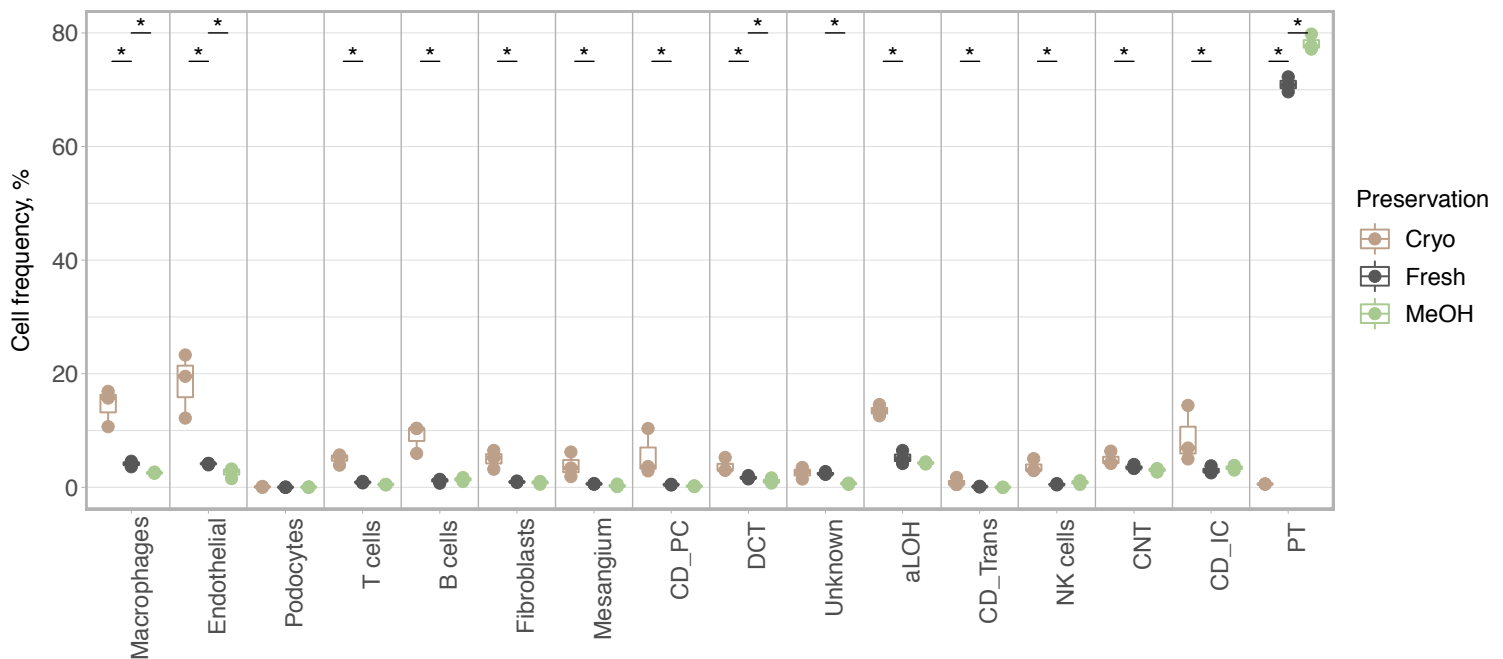
aLOH: ascending loop of Henle; CD_IC: intercalated cells of collecting duct; CD_PC: principal cells of collecting duct; CD_Trans: transitional cells of collecting duct; CNT: connecting tubule; DCT: distal convoluted tubule; PT: proximal tubule.

Fig. S5

Cold dissociation



Warm dissociation

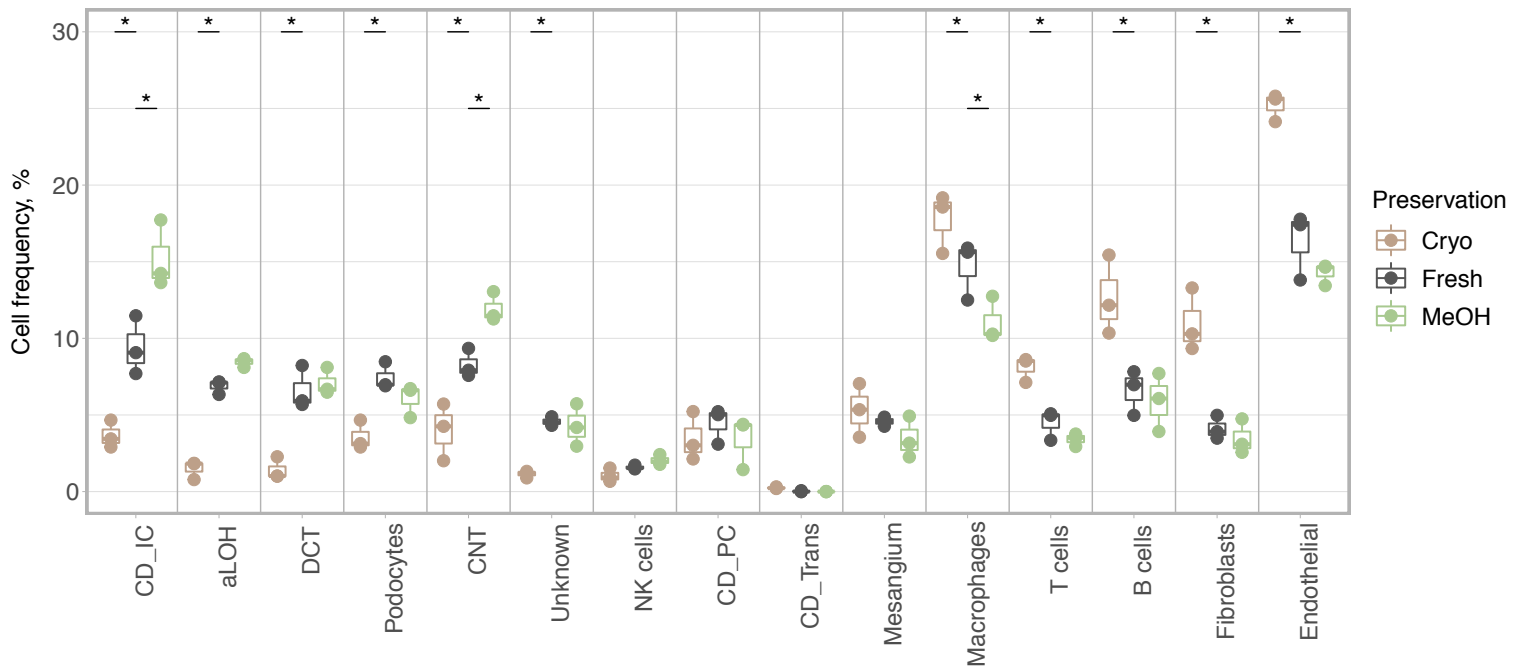


Cell type composition of fresh and preserved kidneys. Three biological replicates are shown per condition. Asterisks denote two-sided chi-square test p-value < 0.001.

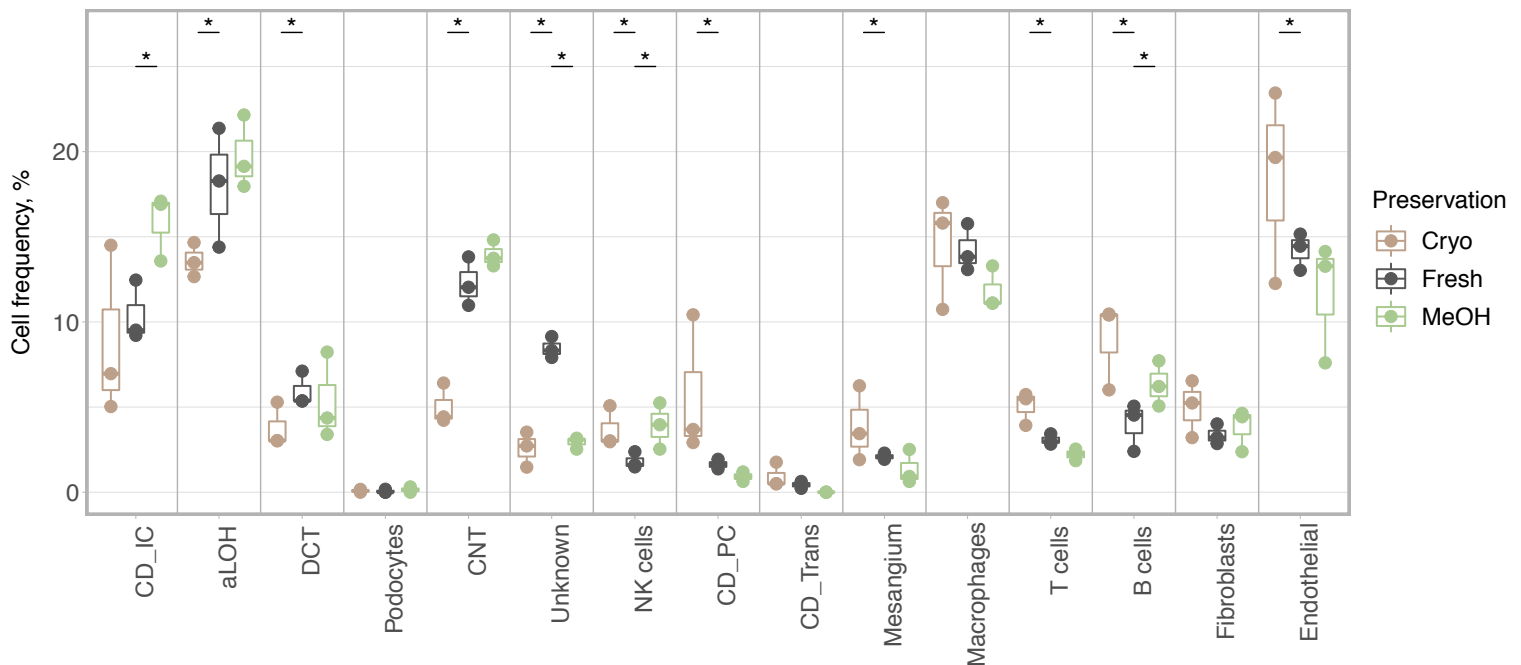
aLOH: ascending loop of Henle; CD_IC: intercalated cells of collecting duct; CD_PC: principal cells of collecting duct; CD_Trans: transitional cells of collecting duct; CNT: connecting tubule; DCT: distal convoluted tubule; PT: proximal tubule.

Fig. S6

Cold dissociation



Warm dissociation

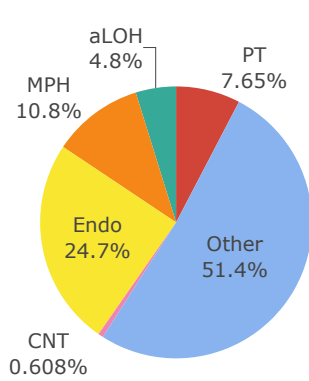


Cell type composition of non-proximal tubule cells in fresh and preserved kidneys. Three biological replicates are shown per condition. Asterisks denote two-sided chi-square test p-value < 0.001.

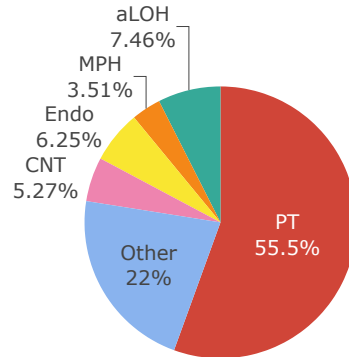
aLOH: ascending loop of Henle; CD_IC: intercalated cells of collecting duct; CD_PC: principal cells of collecting duct; CD_Trans: transitional cells of collecting duct; CNT: connecting tubule; DCT: distal convoluted tubule.

Fig. S7

Cryopreserved



Fresh

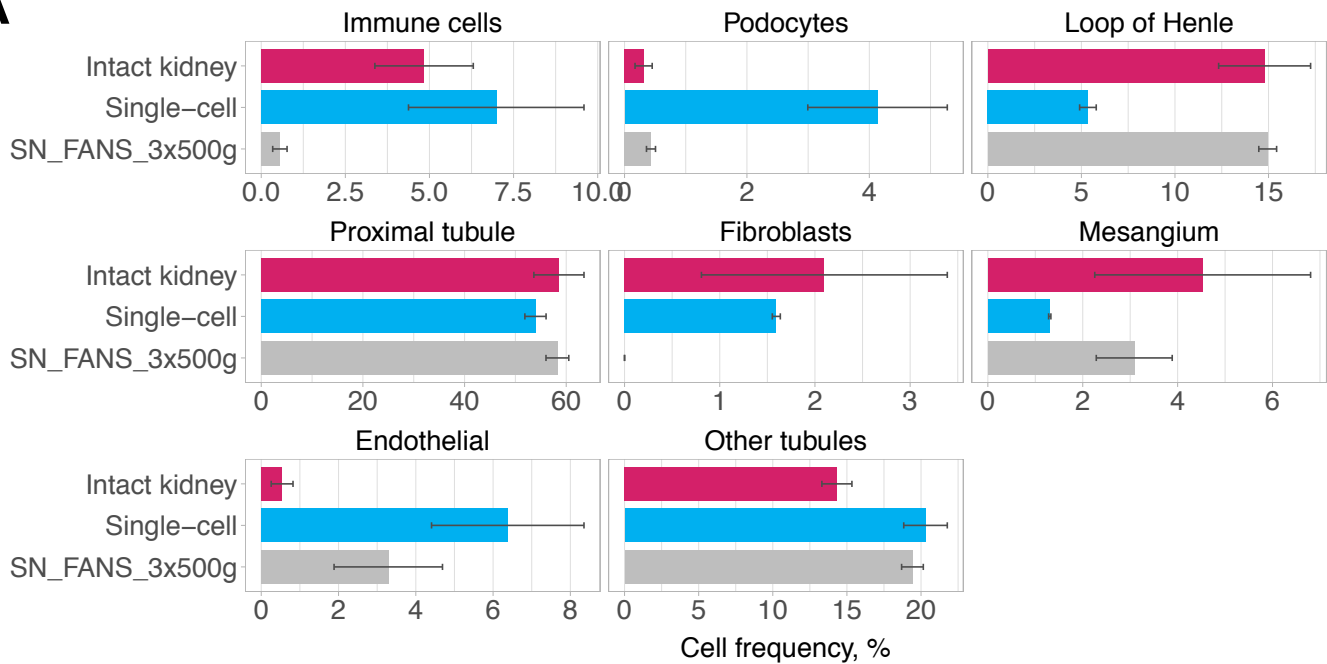


Cell type composition of fresh and cryopreserved cold-dissociated samples in the repeated experiment using Balb/c female mice, 10x v3 chemistry, 2 weeks storage, and 1200g spin.

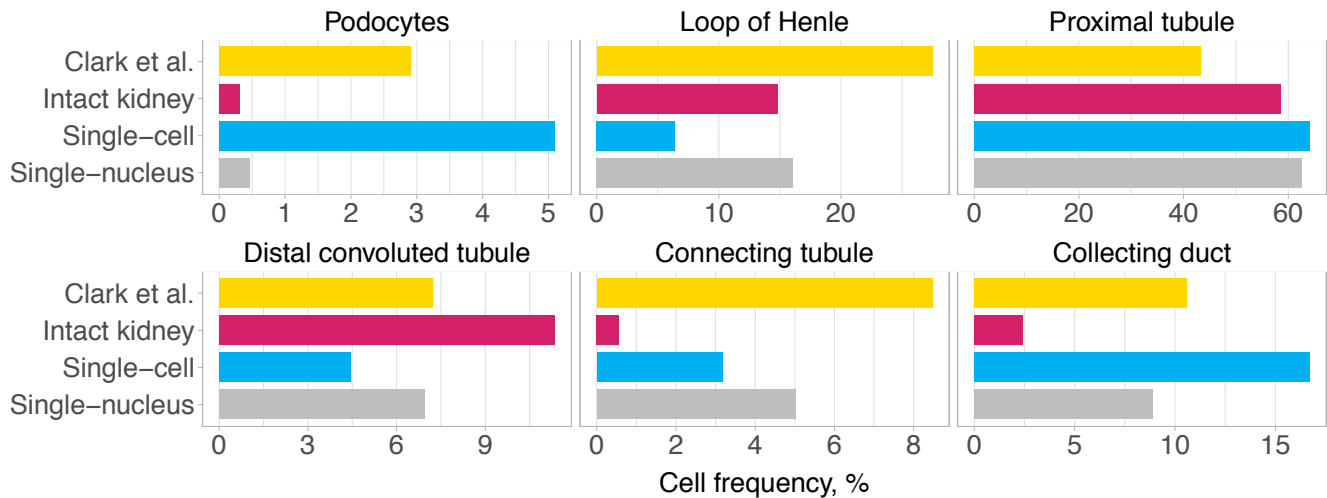
aLOH: ascending loop of Henle; MPH: macrophages; CNT: connecting tubule; PT: proximal tubule.

Fig. S8

A

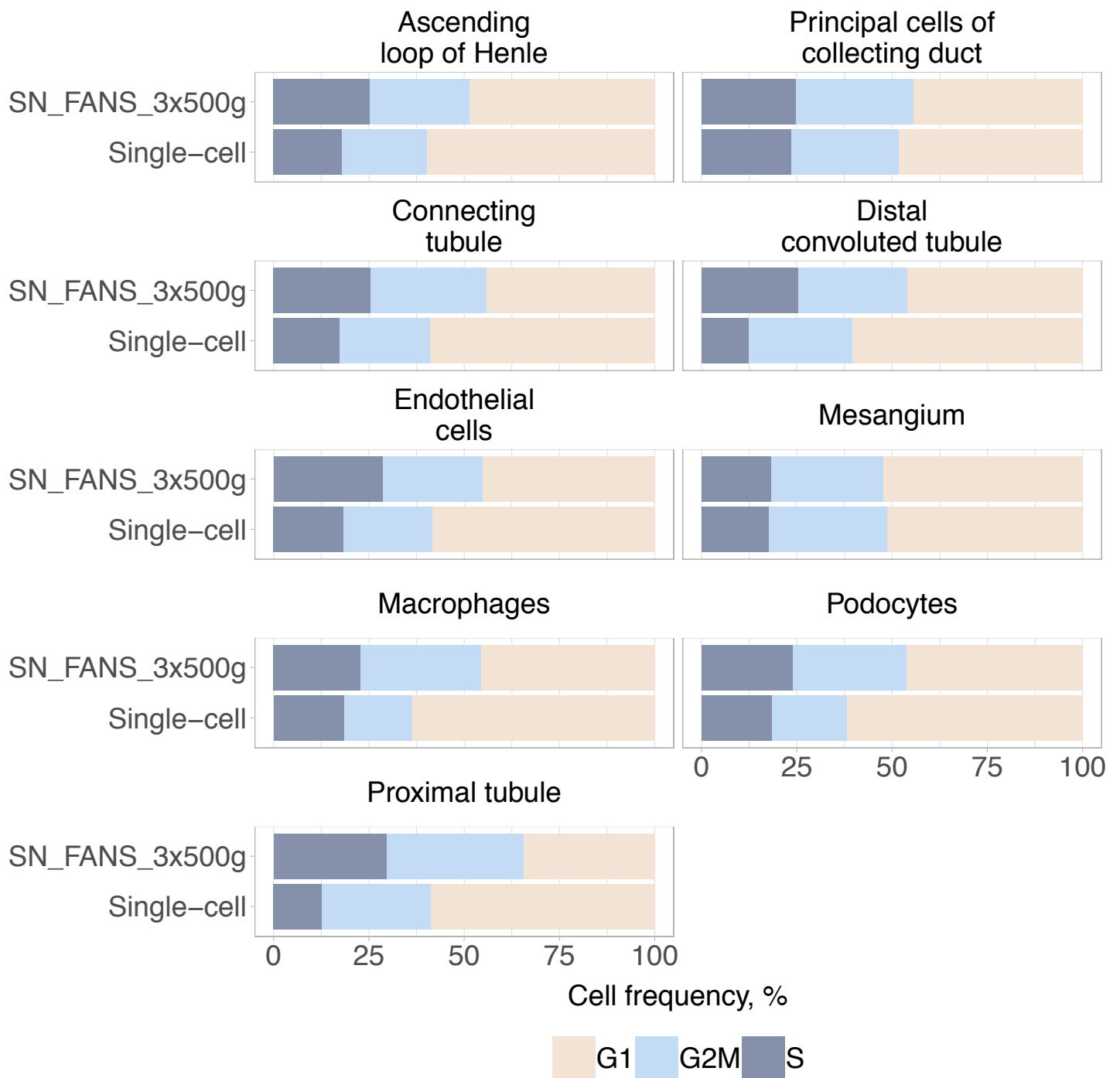


B



Comparison of single-cell and single-nucleus libraries in Balb/c male mice. **a)** Cell type composition for kidneys from Balb/c male mice. Average percentages for scRNA-seq libraries are shown in blue and for snRNA-seq libraries in grey. BSEQ-sc estimates are shown for bulk RNA-seq of intact kidneys. Error bars are standard error of mean. **b)** Abundance of renal epithelial cell types in Clark *et al.* study in comparison to our data from Balb/c male mice.

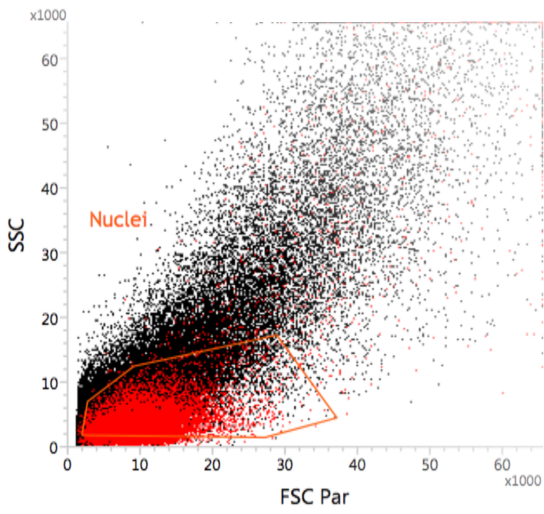
Fig. S9



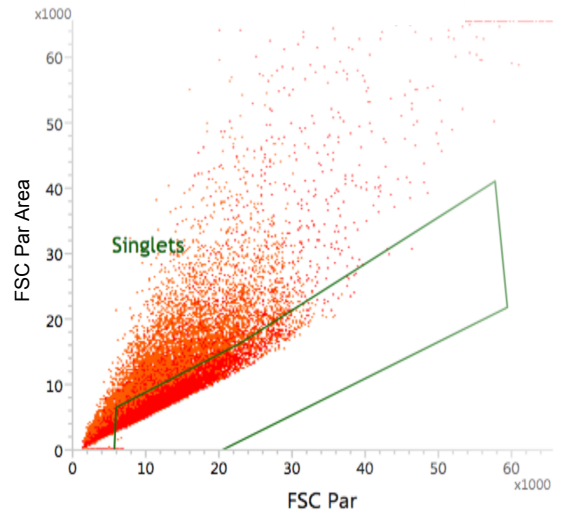
Cell cycle phases inferred in scRNA-seq and snRNA-seq libraries from Balb/c male mice.

Fig. S10

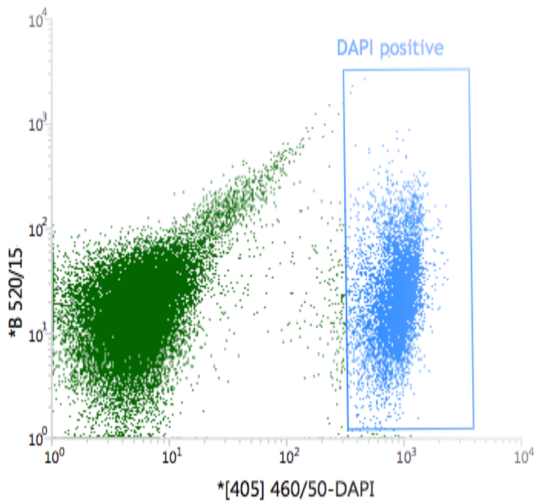
1st gate for nuclei



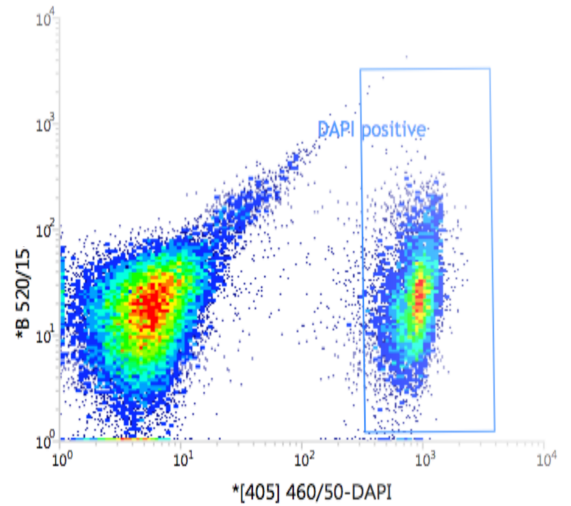
2nd gate for singlets



3rd gate for DAPI+

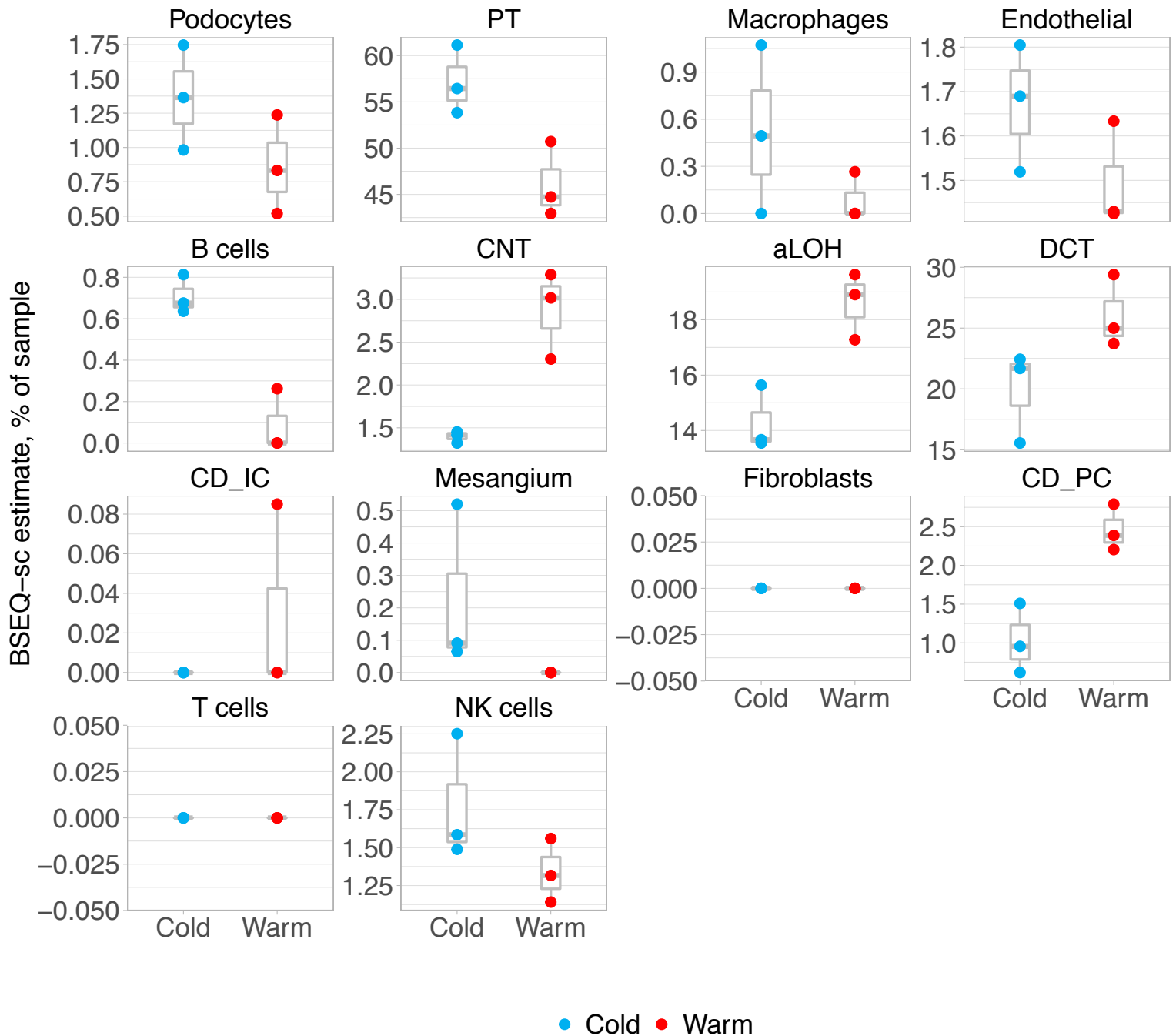


Density plot



FANS gating strategy.

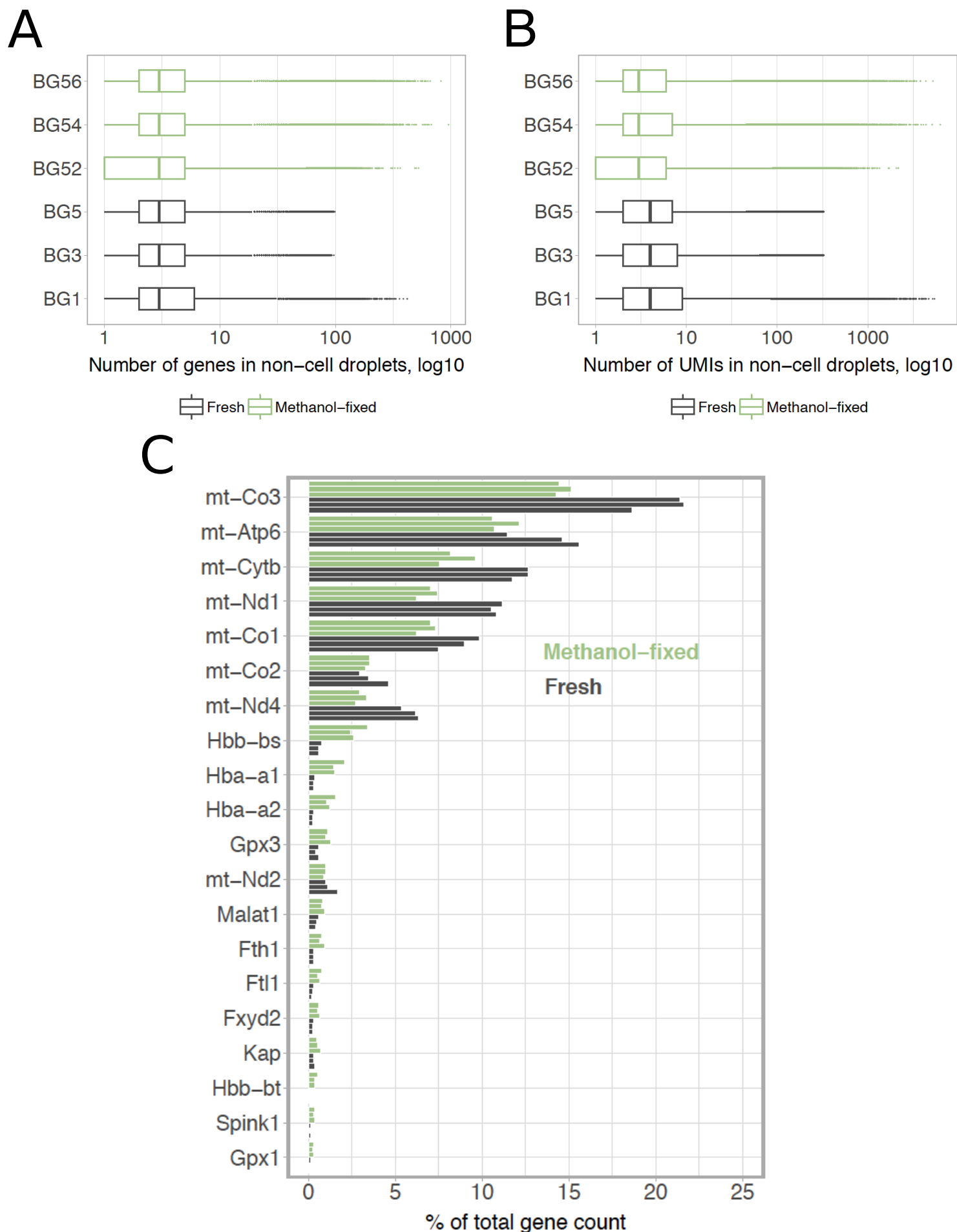
Fig. S11



BSEQ-sc deconvolution of bulk RNA-seq profiles of cold- and warm-dissociated kidney single-cell suspensions. Three biological replicates are shown per condition.

aLOH: ascending loop of Henle; CD_IC: intercalated cells of collecting duct; CD_PC: principal cells of collecting duct; CNT: connecting tubule; DCT: distal convoluted tubule; PT: proximal tubule.

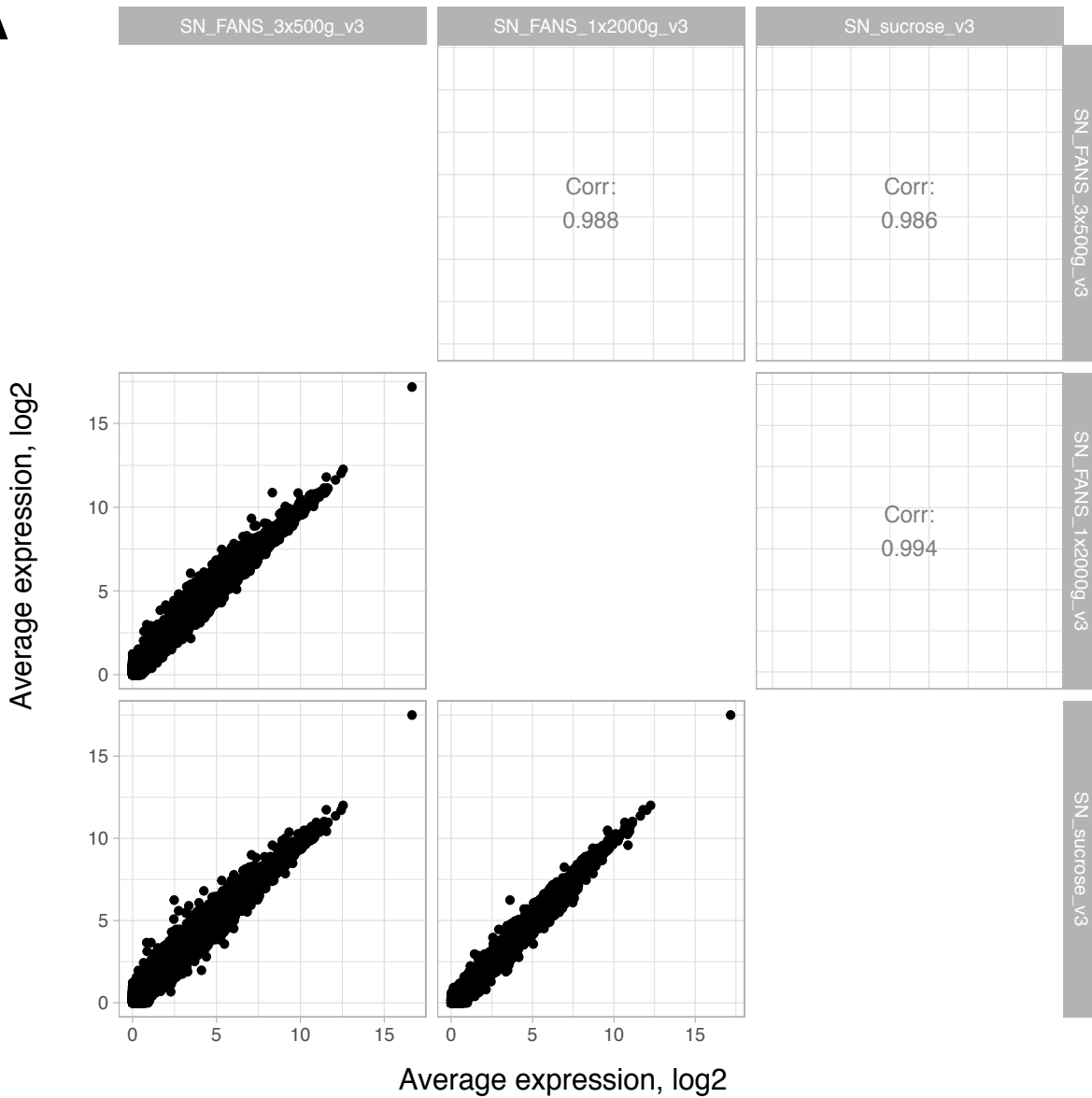
Fig. S12



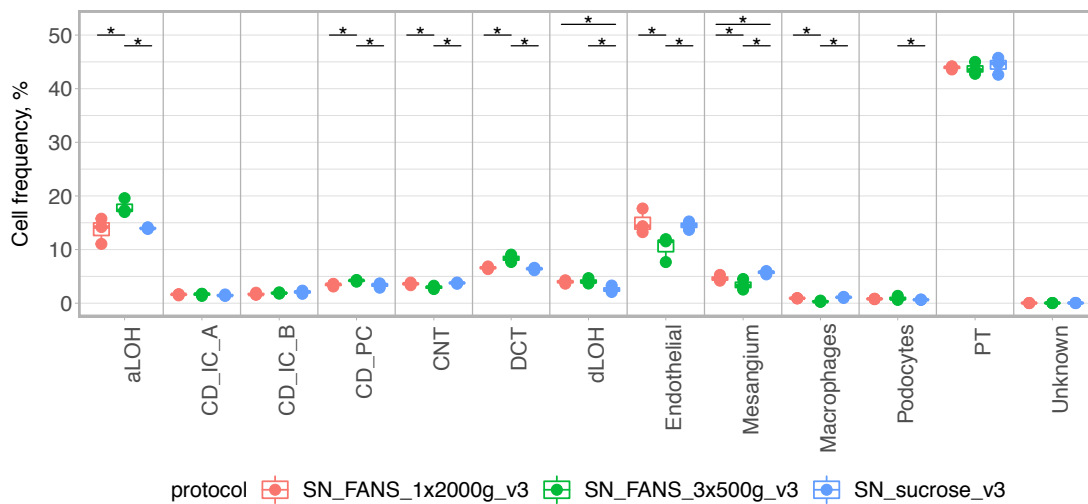
Comparison of ambient RNA contamination in methanol-fixed and freshly profiled aliquots of cold-dissociated samples.

Fig. S13

A



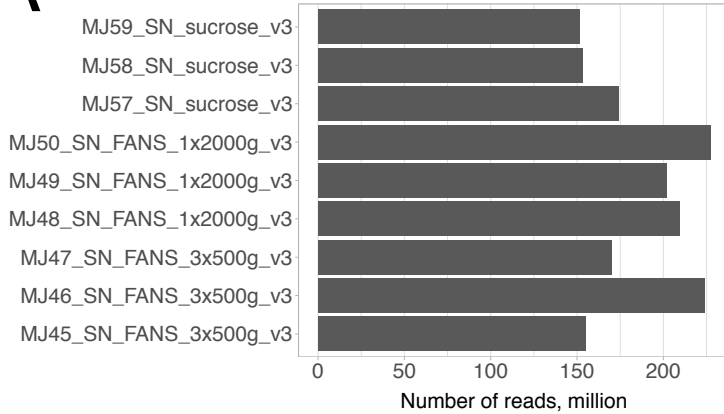
B



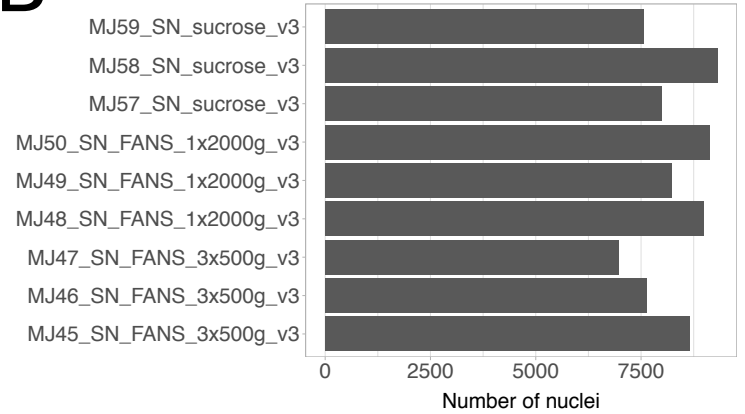
Comparison of nuclei isolation protocols. **a)** Aggregate gene expression and correlation between protocols. Raw counts were summed up for nuclei in each sample separately, then normalised to reads per million, averaged across biological replicates and log₂-transformed with a pseudo count of 1 for plotting. Spearman correlation coefficients are shown. **b)** Cell type composition of the three nuclei isolation protocols. Three biological replicates are shown per protocol. Asterisks denote two-sided chi-square test p-value < 0.001. aLOH: ascending loop of Henle; CD_IC_A: type A intercalated cells of collecting duct; CD_IC_B: type B intercalated cells of collecting duct; CD_PC: principal cells of collecting duct; CNT: connecting tubule; DCT: distal convoluted tubule; dLOH: descending loop of Henle; PT: proximal tubule.

Fig. S14

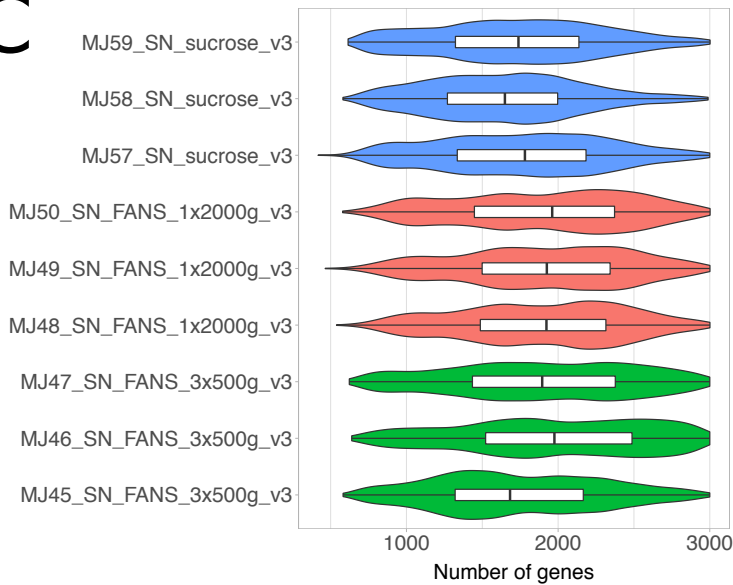
A



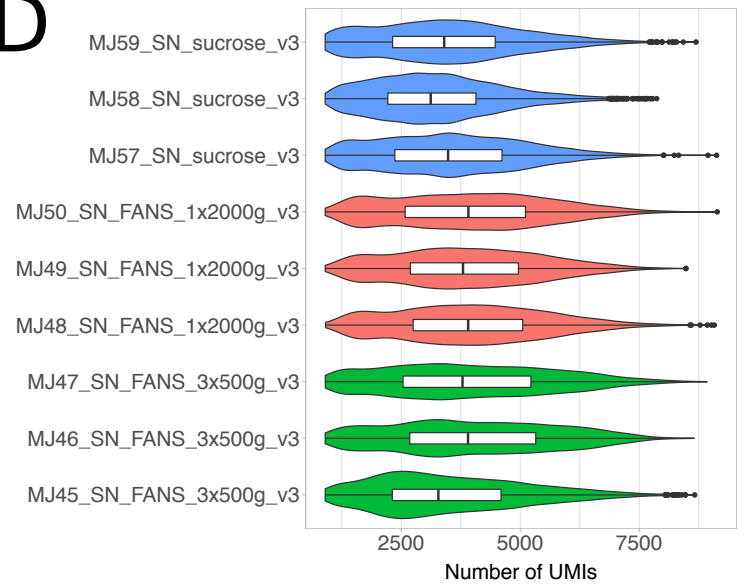
B



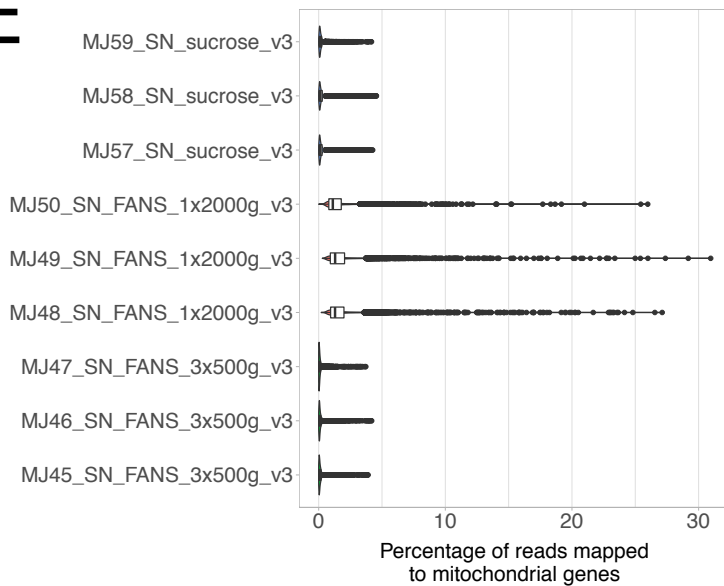
C



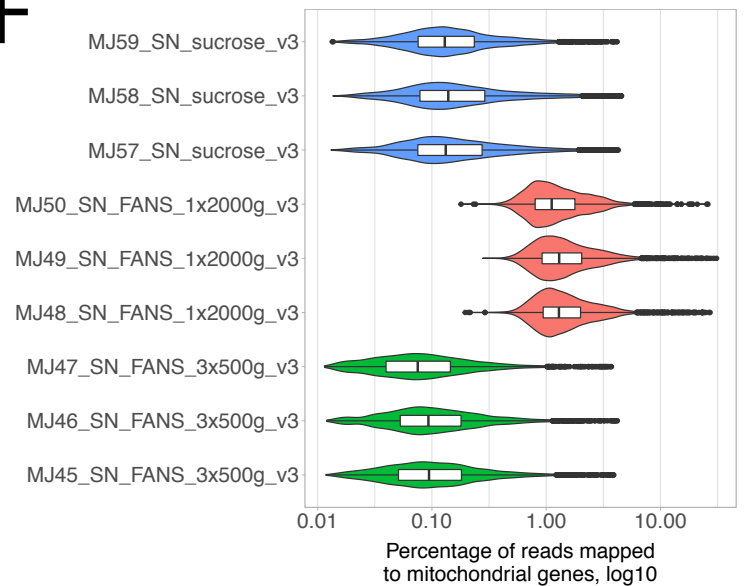
D



E

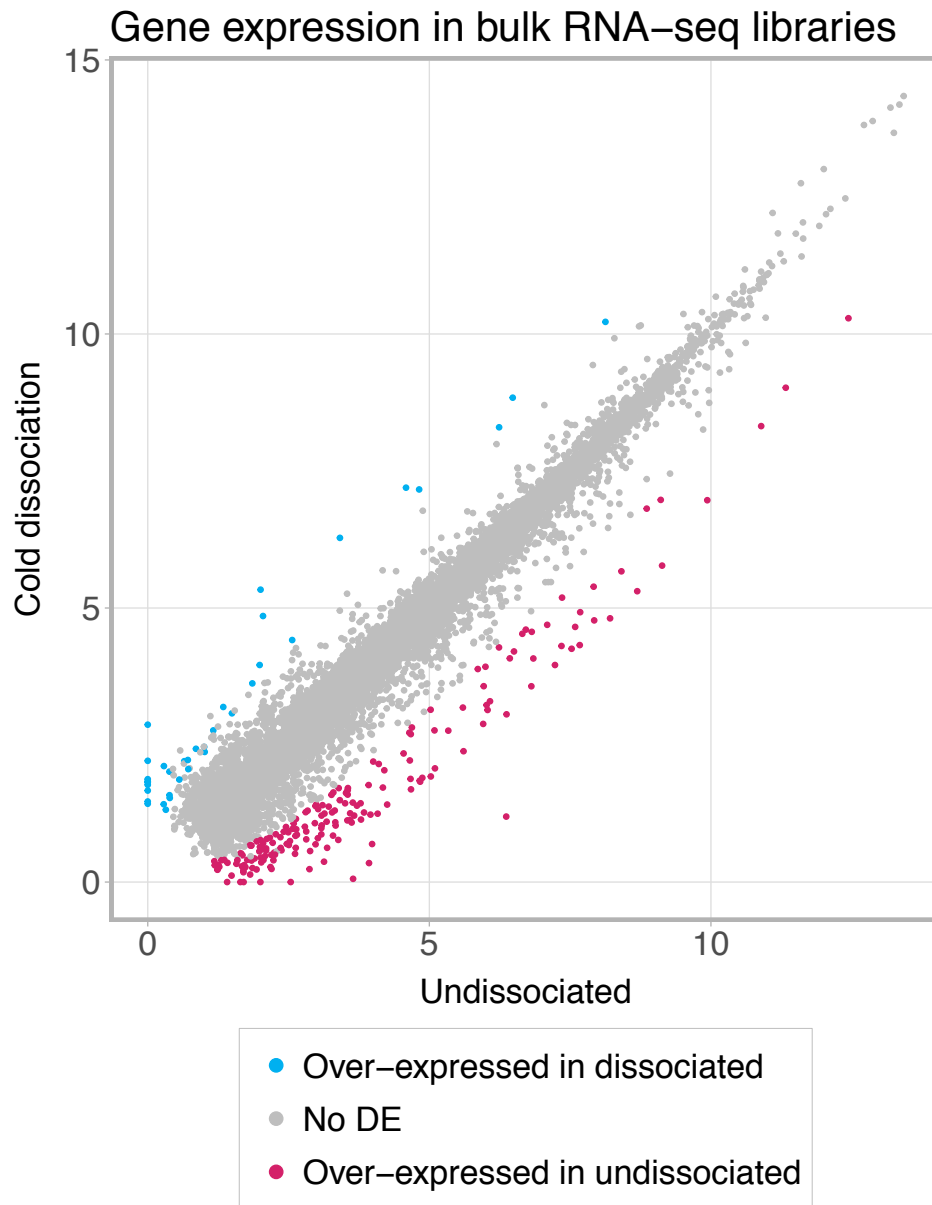


F



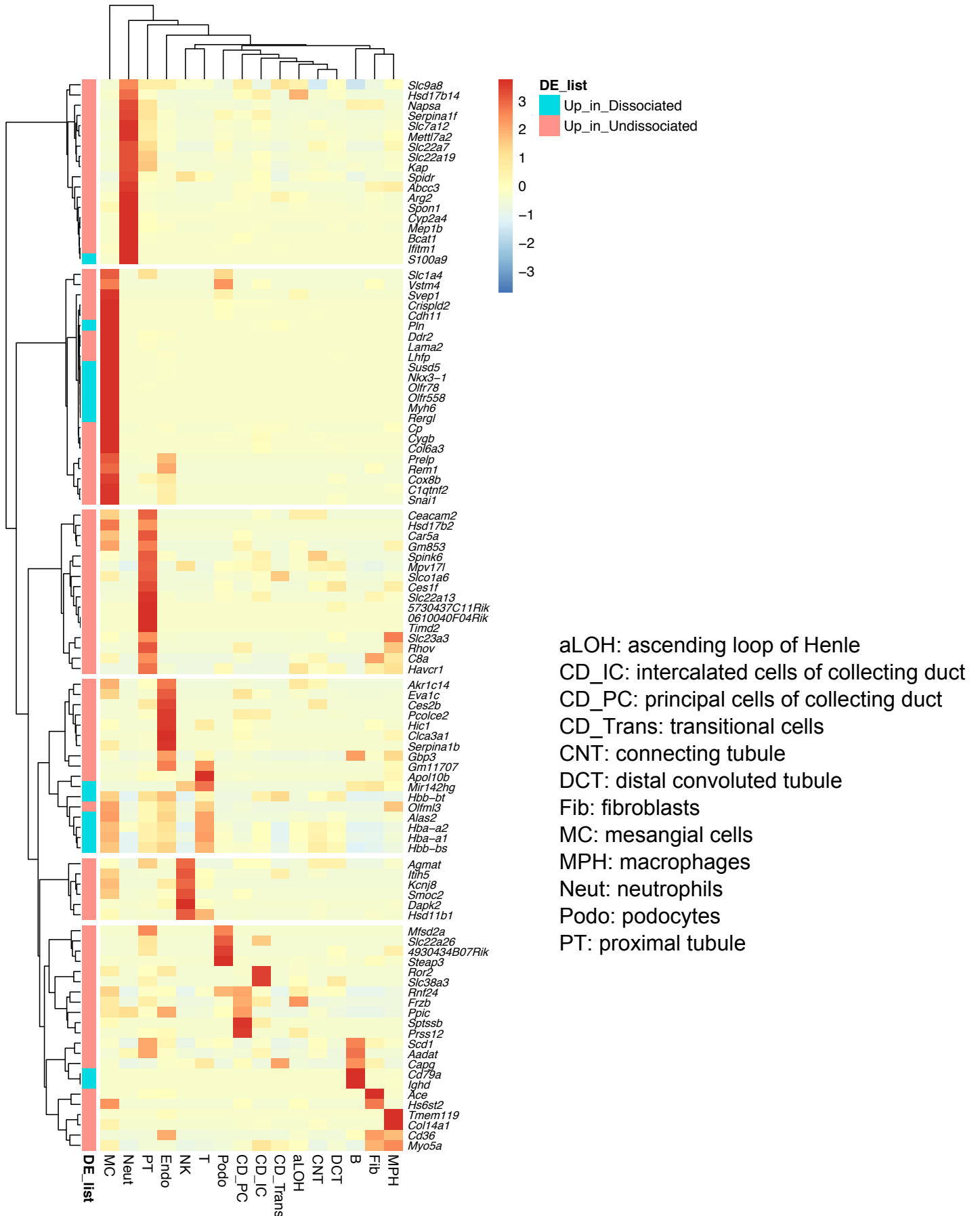
Comparison of nuclei isolation protocols. **a)** Total number of sequenced reads for each library. **b)** Number of nuclei passing all filtering steps as described in **Methods**. **c)** Distribution of the number of genes detected in nuclei. **d)** Distribution of the number of unique molecular identifiers detected in nuclei. **e)**, **f)** Distribution of the percentage of reads mapped to mitochondrial genes.

Fig. S15



Comparison of bulk RNA-seq profiles of intact kidneys and cold-dissociated single-cell suspensions. GeTMM-normalised counts were averaged across three biological replicates and \log_2 -transformed after adding a pseudo count of 1. DEGs identified with $FDR < 0.05$ and \log_2FC threshold of 2 using edgeR exact test are indicated.

Fig. S16



Expression of genes differentially expressed between bulk RNA-seq profiles of intact and dissociated kidneys in the matching single-cell dataset, Balb/c female mice. Normalised counts were averaged for each cell type, rows were scaled for plotting.